

RESEARCH ARTICLE

Open Access

Biogeochemistry and limnology in Antarctic subglacial weathering: molecular evidence of the linkage between subglacial silica input and primary producers in a perennially ice-covered lake

Yoshinori Takano^{1*}, Hisaya Kojima², Eriko Takeda², Yusuke Yokoyama^{1,3} and Manabu Fukui²

Abstract

We report a 6,000 years record of subglacial weathering and biogeochemical processes in two perennially ice-covered glacial lakes at Rundvågshetta, on the Soya Coast of Lützow-Holm Bay, East Antarctica. The two lakes, Lake Maruwan Oike and Lake Maruwan-minami, are located in a channel that drains subglacial water from the base of the East Antarctic ice sheet. Greenish-grayish organic-rich laminations in sediment cores from the lakes indicate continuous primary production affected by the inflow of subglacial meltwater containing relict carbon, nitrogen, sulfur, and other essential nutrients. Biogenic silica, amorphous hydrated silica, and DNA-based molecular signatures of sedimentary facies indicate that diatom assemblages are the dominant primary producers, supported by the input of inorganic silicon (Si) from the subglacial inflow. This study highlights the significance of subglacial water-rock interactions during physical and chemical weathering processes and the importance of such interactions for the supply of bioavailable nutrients.

Keywords: Antarctic ice sheet; Subglacial biogeochemistry; Subglacial limnology; Sedimentary record; Siliceous primary producer

Background

Subglacial Antarctic lakes were first identified by radio-echo sounding in the late 1960s (Robin *et al.* 1970; Oswald and Robin 1973). Since then and especially during the past two decades, researchers have identified numerous subglacial lakes (e.g., Kapitsa *et al.* 1996; Siegert *et al.* 1996; Jouzel *et al.* 1999; Karl *et al.* 1999; Priscu *et al.* 1999; Christner *et al.* 2006) and extensive networks of subglacial meltwater channels in Antarctica (e.g., Anderson *et al.* 2002; Wingham *et al.* 2006). Siegert and coworkers compiled an inventory of 145 subglacial lakes beneath the East Antarctic Ice Sheet and the West Antarctic Ice Sheet (EAIS and WAIS) (Siegert 2000; Siegert *et al.* 2005). The subglacial water, which initially derives from melting caused by geothermal heat (heat flow rates, approximately 50 mW m⁻²; Siegert *et al.*

2012), is involved in various water-rock interaction processes beneath the ice sheet, and these interactions play important roles in the supply of nutrients, including trace metals, to organisms in Antarctic environments. For example, silicon (Si) is one of the critical elements limiting the growth of Antarctic diatoms (e.g., Nelson and Treguer 1992), likewise nitrogen and other elements (e.g., Hutchins and Bruland 1998). Moreover, glacial input of particulate and dissolved Fe is essential to biological productivity in the Southern Ocean (Raiswell and Canfield 2012). In addition to the nutrient contributed by seasonal snowmelt (Hodson 2006), subglacial meltwater flowing through channels may also influence the productivity and diversity of microbial communities by controlling the concentrations of nutrients and the physicochemical conditions of glacial environments (e.g., Tranter *et al.* 2005; Esposito *et al.* 2006; Mikucki *et al.* 2009; Bentley *et al.* 2011).

At the margins of the EAIS and WAIS, there are a number of locations where former subglacial lakes have

* Correspondence: takano@jamstec.go.jp

¹Department of Biogeochemistry, Japan Agency for Marine-Earth Science and Technology (JAMSTEC), 2-15 Natsushima, Yokosuka, Kanagawa 237-0061, Japan
Full list of author information is available at the end of the article

emerged from beneath the ice after the deglaciation since the Last Glacial Maximum (LGM, ca. 20 ka; Yokoyama and Esat 2011; lake settings, e.g., Hodgson *et al.* 2006; Hodgson *et al.* 2009; Verleyen *et al.* 2011). Glacial lakes affected by the input of subglacial water can be observed at the retreating margins of the Antarctic ice sheet. In the Rundvågshetta area on the Soya Coast of Lützow-Holm Bay, East Antarctica (Figure 1a), freshwater flows from the subglacial drainage channels of the EAIS (Anderson *et al.* 2002, and literature therein). The objective of this study was to examine the interactions between the limnology of the subglacial water input and microbiological responses to the subglacial water discharged into a perennially ice-covered glacial lake at Rundvågshetta (i.e., Lake Maruwan Oike) over the last 6,000 years. By combining geochemical data and the molecular signatures preserved in sediment core samples, this study aimed to clarify the primary factors controlling biological facies patterns in subglacial-water-fed lakes.

Methods

Geological setting of the sampling sites

Since the initial work by Yoshikawa and Toya (1957) and Murayama (1977), studies undertaken in the Lützow-Holm Bay area of East Antarctica have contributed further insight into the limnology of Antarctic lakes and the relative sea-level changes that occurred during the Holocene. Imura *et al.* (2003) described a range of lake types in the Soya Coast region, including freshwater lakes affected by continental glaciers and saline lakes that evaporated after their isolation from seawater during the Holocene glacio-isostatic uplift. Kudoh and Tanabe (2014) reviewed the limnology and ecology of benthic microbial assemblages from saline to glacial lakes in this area. The Holocene marine limit along the Soya Coast is estimated to have been approximately 18 m above the mean sea level (AMSL), based on radio-carbon analyses of *in situ* bivalve fossils from raised beach deposits (*Laternula elliptica*; Miura *et al.* 1998). Cosmogenic-radionuclide-based dating of raised beach exposures showed that Holocene deglaciation occurred locally on the Soya Coast at ca. 10 ka (Yamane *et al.* 2011). Bassett *et al.* (2007) also compared predictive models of glacio-isostatically induced relative sea-level changes at seven other locations around the Antarctic coast, as well as on the Soya Coast.

Rundvågshetta (69°54.5' S, 39°02' E; Figure 1a) is a rock headland at the southwest margin of the Rundvåg Glacier (e.g., Sawagaki and Hirakawa 1997; Miura *et al.* 1998). Figure 1b shows the electric conductivity (mS m⁻¹) of the study site, confirming the origin of the lake water inflow. Two lakes on the headland, Lake Maruwan Oike (hereafter, L. Maruwan), with a water level 8 m AMSL (data

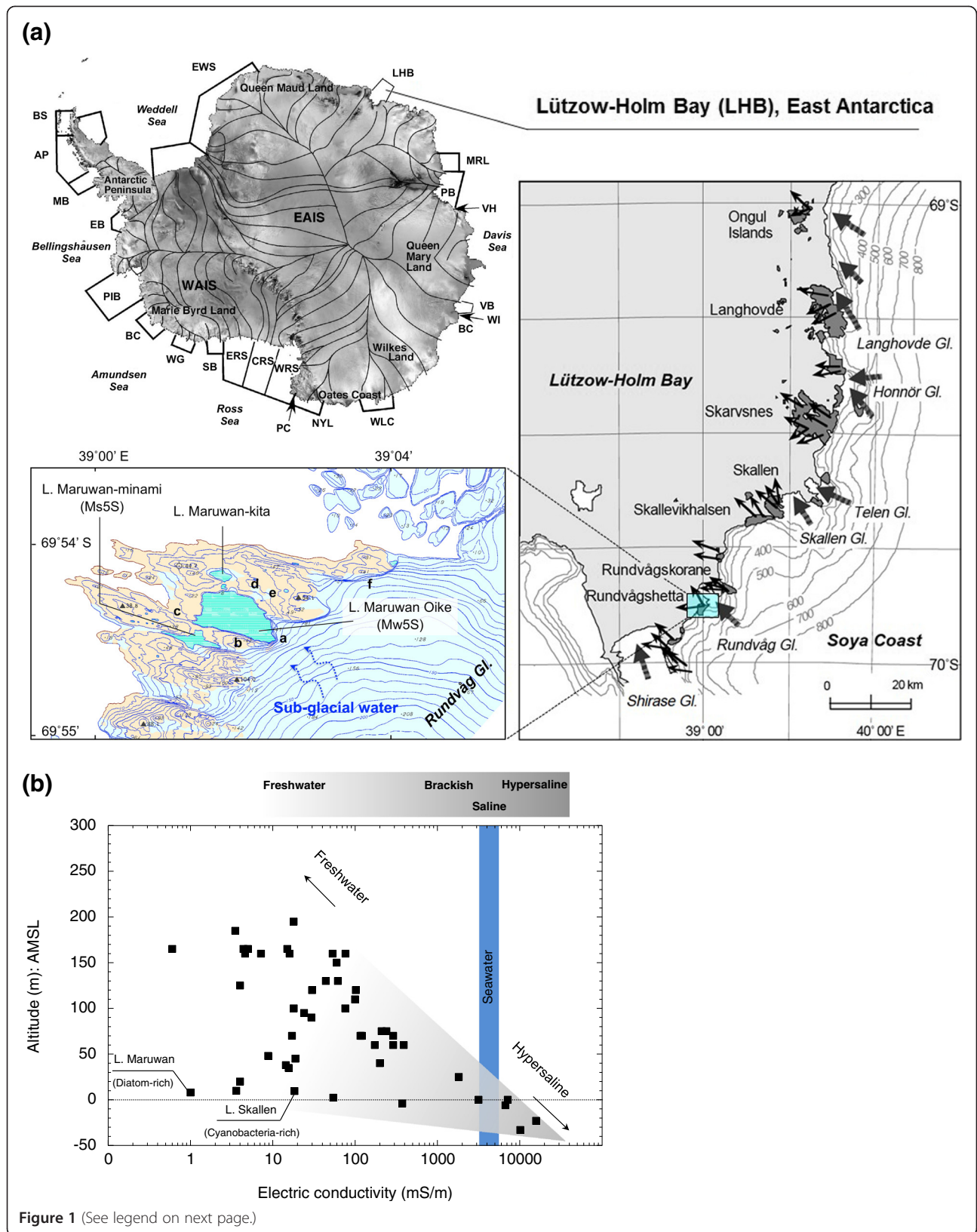
from the Geographical Survey Institute 1984), and Lake Maruwan-minami (hereafter, L. Maruwan-minami), with a water level >8 m AMSL (the overflow channel of L. Maruwan-minami flows into L. Maruwan; see Figure 2a), provide interesting localities in which to evaluate the influence of subglacial water input on the biogeochemical and sedimentological characteristics of the lakes into which it is discharged (Table 1). It has been reported that the maximum thickness of the surface ice in the Soya Coast region is less than 2 m (Imura *et al.* 2003). Figure 2 shows lakes Maruwan and Maruwan-minami and the surrounding features, including Rundvåg Glacier, a lateral moraine close to the glacier, and the outflows of lakes Maruwan and Maruwan-minami. We also observed a number of erratic boulders derived from glacial transport processes.

Lacustrine sediments were collected using push-type corers (diameter, < 8 cm; see the core images in Figure 3) during the 47th Japanese Antarctica Research Expedition (December 2005). The latitude and longitude of the sampling position in L. Maruwan (hereafter, sample Mw5S; core length, 156 cm) were recorded with GPS as 69.54°27.7' S and 39.02°46.7' E, respectively. The water depth and the ice thickness at this site were 20.2 and 1.5 m, respectively (cf. surface sediment description; Watanabe *et al.* 2013). We also collected lake sediments from L. Maruwan-minami (hereafter, sample Ms5S) as a reference site (see Additional file 1). The cores were cut into 3 to 10 cm intervals (to fit into the field refrigeration unit) and stored at 0 to 4°C for later geochemical analysis and at -20°C for later molecular analysis.

Geochemical analysis of sedimentary facies

The major elements (MgO, Al₂O₃, SiO₂, K₂O, CaO, TiO₂, MnO, and Fe₂O₃) were analyzed with X-ray fluorescence (XRF; JEOL JSX-3211; JEOL Ltd., Tokyo Japan), following Takano *et al.* (2012), and calibrated to Geological Survey of Japan (GSJ) standards (JA-1, JA-3, JB-1a, JB-3, JG-2, JG-3, JGb-1, JP-1, JLK-1, JLS-1, JDO-1, JSI-1, JCh-1, JR-3, JMn-1, JSd-2, and JSd-3; Imai *et al.* 1995, 1999). The data presented represent the average values of duplicate analyses. Amorphous hydrated silica (opal-A) identified with X-ray diffraction (XRD; Mac Science Co., Ltd., Yokohama, Japan) was used as a proxy for amorphous biogenic silica derived from diatoms (siliceous primary producers; e.g., Kastner *et al.* 1977; Leng and Barker 2006), with DNA-based molecular signatures as supporting data (Takano *et al.* 2012). Color data were obtained with a digital color meter (Konica Minolta, Tokyo, Japan; SPAD 503) and revised Standard Soil Color Charts (Oyama and Takehara 2005).

The methods used for elemental and bulk isotopic analyses are described by Takano *et al.* (2012). Briefly, the analyses of carbon, nitrogen, and sulfur were performed



(See figure on previous page.)

Figure 1 Drainage map of the Antarctic Ice Sheet and electric conductivity (mS m^{-1}) of the study site. (a) (upper left) Drainage map of the Antarctic Ice Sheet showing areas where marine and geological surveys are being conducted to record the extent of the Last Glacial Maximum (LGM). (right) Detail of the Soya coast, Lützow-Holm Bay, East Antarctica, showing the locations of ice-covered (white) and ice-free (shaded) areas at Rundvågshetta, Skallen, Skarvsnes, and Langhovde. Arrows show the flow directions of the present outlet glaciers (after Sawagaki and Hirakawa 1997). (lower left) Topography at Rundvågshetta, showing the locations of lakes Maruwan, Maruwan-minami, and Maruwan-kita. Labels a to f indicate the locations of the images in Figure 2. NWWWS, northwestern Weddell Sea; BS, Bransfield Strait; AP, Antarctic Peninsula; MB, Marguerite Bay; EB, Eltanin Bay; PIB, Pine Island Bay; BC, Bakutis Coast; WG, Wrigley Gulf; SB, Sulzberger Bay; WRS, Western Ross Sea; CRS, Central Ross Sea; ERS, Eastern Ross Sea; NVL, Northern Victoria Land; WLC, Wilkes Land Coast; PC, Pennell Coast; BC, Budd Coast; WI, Windmill Islands; PB, Petersen Bank; VB, Vincennes Bay; VH, Vestfold Hills; PB, Prydz Bay; MRL, Mac. Robertson Land; LHB, Lützow-Holm Bay; EWS, eastern Weddell Sea; SWS, southwestern Weddell Sea (modified from Anderson *et al.* 2002). (b) Diagram showing the altitudes of lakes (in meters above the mean sea level; AMSL) on the Soya Coast and electrical conductivities of lake waters (in mS/m) obtained by Imura *et al.* (2003), combined with data from L. Maruwan (diatom-rich microflora; this study) and L. Skallen (cyanobacteria-rich microflora; Takano *et al.* 2012). Note that the altitude data for L. Maruwan (8.0 m) and L. Skallen (9.64 ± 0.02 m) were referred from Geographical Survey Institute (1984) and Takano *et al.* (2012), respectively. See the limnological features for the numbers of lakes (Kudoh and Tanabe 2014). Seawater electrical conductivity (e.g., Cox *et al.* 1967; Lee *et al.* 2006), salinity (e.g., Koblinsky *et al.* 2003), and a variety of electrical conductivity measurements in hypersaline lakes (e.g., Williams and Sherwood 1994) are also given.

using a Micro CORDER JM10 (J-Science Lab Co., Ltd, Kyoto, Japan). Carbon and nitrogen isotopic ratios were determined using an elemental analyzer (Costech 4010 or Flash 2000)-isotope ratio mass spectrometer (Thermo Finnigan, Delta Plus, or Thermo Finnigan Delta V Advantage). Carbon and nitrogen isotopic compositions are expressed as per mil (‰) deviations from the standard as:

$$\delta^{13}\text{C} = \left[\left(\frac{^{13}\text{C}/^{12}\text{C}}{^{13}\text{C}/^{12}\text{C}} \right)_{\text{sample}} / \left(\frac{^{13}\text{C}/^{12}\text{C}}{^{13}\text{C}/^{12}\text{C}} \right)_{\text{standard}} - 1 \right] \times 1,000 (\text{‰ vs. PDB})$$

$$\delta^{15}\text{N} = \left[\left(\frac{^{15}\text{N}/^{14}\text{N}}{^{15}\text{N}/^{14}\text{N}} \right)_{\text{sample}} / \left(\frac{^{15}\text{N}/^{14}\text{N}}{^{15}\text{N}/^{14}\text{N}} \right)_{\text{standard}} - 1 \right] \times 1,000 (\text{‰ vs. Air}),$$

respectively.

The standard deviations for the carbon and nitrogen isotopic compositions obtained using authentic standard reagents (cf. Tayasu *et al.* 2011) were as follows: BG-A ($n = 12$, $\delta^{13}\text{C} < \pm 0.26\text{‰}$, $\delta^{15}\text{N} < \pm 0.25\text{‰}$), BG-P ($n = 6$, $\delta^{13}\text{C} < \pm 0.05\text{‰}$, $\delta^{15}\text{N} < \pm 0.24\text{‰}$), and BG-T ($n = 9$, $\delta^{13}\text{C} < \pm 0.08\text{‰}$, $\delta^{15}\text{N} < \pm 0.26\text{‰}$) in the first validation and BG-A ($n = 10$, $\delta^{13}\text{C} < \pm 0.12\text{‰}$, $\delta^{15}\text{N} < \pm 0.26\text{‰}$), BG-P ($n = 6$, $\delta^{13}\text{C} < \pm 0.06\text{‰}$, $\delta^{15}\text{N} < \pm 0.18\text{‰}$), and BG-T ($n = 7$, $\delta^{13}\text{C} < \pm 0.11\text{‰}$, $\delta^{15}\text{N} < \pm 0.38\text{‰}$) in the second validation. Some of the organic carbon fractions extracted after HCl pretreatment were analyzed to obtain radiocarbon age data, corrected for the $\delta^{13}\text{C}$ value, using an accelerator mass spectrometer (AMS) at the University of Tokyo, Japan (Yokoyama *et al.* 2007), or at Beta Analytic Inc., Florida, USA.

DNA-based analyses

DNA was analyzed in 18 sections (0 to 2, 2 to 4, 4 to 6, 8 to 10, 13 to 14, 14 to 16, 22 to 24, 30 to 32, 38 to 40, 49 to 52, 52 to 55, 55 to 58, 58 to 61, 61 to 64, 78 to 80, 95 to 100, 115 to 120, and 135 to 140 cm) of the core sample obtained from L. Maruwan; DNA was extracted from a 0.5 to 1.0 g sample from each section using an UltraClean Soil DNA Isolation Kit (Mobio, Carlsbad,

CA, USA). Polymerase chain reaction (PCR) amplification of the 16S rRNA gene, denaturing gradient gel electrophoresis (DGGE), and sequencing of the resulting DGGE bands were performed as described previously (Muyzer *et al.* 1996; Takano *et al.* 2012). The sequences were taxonomically identified with the RDP Classifier from the Ribosomal Database Project-II release 11.

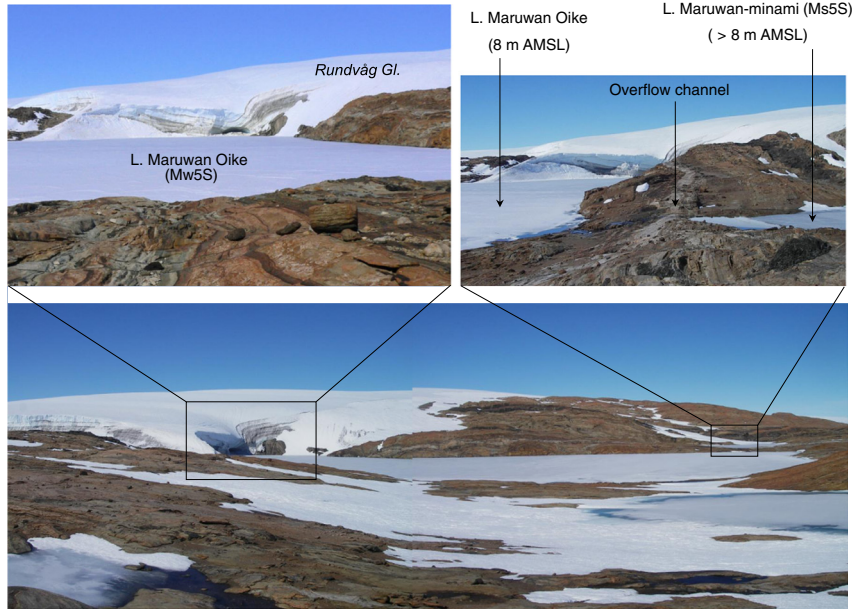
Results

Geochemistry, major elemental compositions, and sedimentary facies

The olive-gray, olive-black, and dark olive-gray laminations in the upper sections of core Mw5S from L. Maruwan are the remains of soft microbial mats. The laminations in the lower sections of the core are largely gray to olive-black (Figure 3a). The distinct laminations represent conditions favorable for preservation (i.e., no bioturbation). Some sediment deformation was observed at depths of 0 to 5, 10, and 50 to 60 cm. The lithological descriptions and the corresponding ^{14}C ages of organic carbon (years BP) are shown in Figure 3b. Geochemical analyses of carbon, nitrogen, sulfur, and major elements were used to identify the sedimentary facies.

Figure 4a shows depth profiles of the concentrations of the major elements and the carbon and nitrogen isotope ratios. Total carbon (TC) and the carbon isotopic composition ($\delta^{13}\text{C}$) of bulk organic matter ranged from 0.7 to 3.5 wt% (mean, 2.6 ± 0.6 wt%) and from -17.0‰ to -23.6‰ (vs. PDB), respectively. Total nitrogen (TN) and the nitrogen isotopic composition ($\delta^{15}\text{N}$) of the bulk organic matter were <0.48 wt% (mean, 0.3 ± 0.1 wt%) and from $+2.2\text{‰}$ to $+6.6\text{‰}$ (vs. Air), respectively. Total sulfur (TS) ranged from 0.3 to 1.6 wt% (mean, 1.0 ± 0.3 wt%). The profiles show that the increasing trends in carbon and nitrogen with the movement from marine to freshwater facies in L. Skallen and L. Oyako (Takano *et al.* 2012; Matsumoto *et al.* 2014) are not observed in L. Maruwan. The sedimentary facies were not distinguishable on the basis of their nitrogen isotopic

(a) Landscape around L. Maruwan Oike



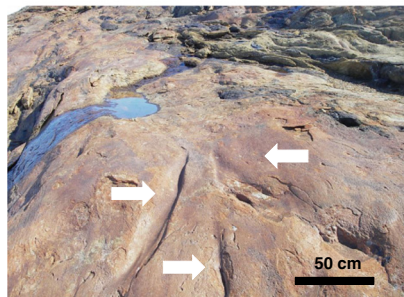
(b) Lateral moraine



(c) Outflowing from L. Maruwan



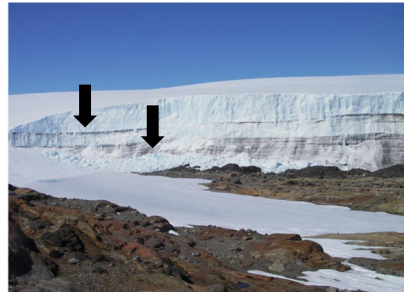
(d) Possible past sub-glacial erosion



(e) Erratic boulders and modern microbial mat



(f) Colored glacial layer in the edge



(g) Ice-cave structure beneath the glacier



Figure 2 (See legend on next page.)

(See figure on previous page.)

Figure 2 Terrain in the study area, showing lakes Maruwan, Maruwan-minami, and Maruwan-kita and associated geomorphic features.

The locations of the images are shown by labels a to g in Figure 1a (lower left panel). **(a)** Overall features of the study area, showing the proximity of the lakes to Rundvåg Glacier, and the overflow points of lakes Maruwan and Maruwan-minami. **(b)** Lateral moraine close to Rundvåg Glacier. **(c)** Outflow of L. Maruwan. **(d)** Possible subglacial erosion features (after Sawagaki and Hirakawa 1997). **(e)** Present-day microbial mat (dark area) and erratic boulders transported and deposited by past glaciers. **(f)** Exposed stratification in glacial ice. **(g)** Detail of (a), showing a cave-like structure beneath the glacier.

compositions because of the relic nitrogen inputs from subglacial water ($\delta^{15}\text{N}$ up to +6.6‰ in Mw5S; cf. L. Skallen, in the supporting data of Matsumoto *et al.* 2010).

The trends in the contents of some major elements indicate a marked transition from marine to lacustrine conditions in each of the cores (Figure 4a). The sediments deeper than 50 cm depth in the Mw5S core were substantially enriched in SiO_2 (<83%), indicating high SiO_2 end-member values under marine conditions and low SiO_2 values under freshwater conditions. The mixture of these two end-members can be illustrated on SiO_2 - Al_2O_3 and SiO_2 - Fe_2O_3 diagrams, in which contrasting mixing trends are observed (Figure 4b,c). The mixing profiles in these diagrams are similar to those of the reference sample obtained from L. Maruwan-minami (Ms5S; Additional file 1), which is located nearby. The $\text{Al}_2\text{O}_3/\text{TiO}_2$ and $\text{Fe}_2\text{O}_3/\text{TiO}_2$ ratios (Figure 4d) provide information about the source rocks (Young and Nesbitt 1998) episodic hydrological surge events (at 0 to 5 and 50 to 60 cm) and subglacial discharge variations (e.g., Brown 2002).

X-ray diffraction analyses of the sediments from core Mw5S indicate that opal-A is abundant throughout the section, except at 0 to 5 cm, suggesting that the silicate is of biogenic origin (Figure 5). To confirm this observation, we also obtained DNA-based molecular evidence of biogenic signatures (see Figure 5c). The high end-member SiO_2 concentrations, which also suggest large contributions of biogenic silica to the sediments, were probably derived from abundant diatoms (cf. determination of opal-A in the discussion).

Radiocarbon age determinations of sedimentary organic matter

We determined the AMS radiocarbon (^{14}C) ages of the organic matter in the core samples (Figure 3b and Table 2). The ^{14}C values (years BP) at the top of the core ($1,350 \pm 40$ years in Mw5S at a depth of 0 to 2 cm) indicate significant inputs of relic carbon. Therefore, the sediment age at the top of the core of 1,300 years was subtracted from the raw values to calibrate the radiocarbon dates with the corresponding calendar ages (after Berkman and Forman 1996; Miura *et al.* 2002). Similarly, marine benthic organisms have yielded ^{14}C ages of $1,010 \pm 110$ to $1,190 \pm 90$ years BP along the Soya Coast, as reported by Yoshida and Moriwaki (1979). Using this protocol, we estimated the age at which the first sediments were deposited in the bedrock-scoured

glacial basin of L. Maruwan (Figures 1 and 4a) to be at least 4,807 to 5,204 cal BP (2σ). Based on the major elemental compositions (Figure 4b), we also obtained an emergence age (i.e., the transition from marine to freshwater) of 3,382 to 3,560 cal BP (2σ); the median age of 3,471 cal BP occurs at a depth of 46 to 49 cm. Here, we note the possibility that the period from 4,000 to 1,350 cal BP represented a hiatus in the sedimentation processes in L. Maruwan. The sedimentary facies in L. Maruwan-minami, in contrast, did not show a similar profile (Additional file 1). Assuming the continuous inflow of subglacial water, the transitions from marine to freshwater conditions *via* temporary brackish conditions are indistinct in the L. Maruwan cores compared with the transitions observed at lakes Skallen and Oyako, also located on the Soya Coast (Takano *et al.* 2012).

Preliminary results for biological facies and molecular signatures from DGGE analysis

A PCR-DGGE analysis was performed to assess the shifts in the composition of residual DNA in the sediments of L. Maruwan (Figure 5c). Depth-related changes were apparent in regions shallower than 6 cm. In the layers deeper than 4 cm, two predominant bands (labeled with arrows in Figure 5c) were consistently observed throughout the range analyzed. The nucleotide sequences of the two bands were identical, corresponding to the chloroplasts of the marine diatom *Chaetoceros*, and were also identical to the diatom sequence detected in the deeper sediment layers of L. Skallen (Takano *et al.* 2012). The other sequenced DGGE bands (labeled with triangles in Figure 5c) represented taxa of nonphototrophic bacteria determined with a 16S rRNA analysis (unpublished data).

Discussion

Primary producers and estimates of biogenic silica

The lake sediments in core Mw5S (L. Maruwan) record a continuous input of relic carbon, nitrogen, and bioavailable silica from subglacial water, indicated by their chemical constituents, including major elements and isotopes. Hodson *et al.* (2010) experimentally verified the chemical weathering and solute production processes in Antarctic glacial meltwater based on aspects of water-rock interactions and hydrochemistry. Stumpf *et al.* (2012) and Tranter *et al.* (2005) also suggested the important influence of subglacial weathering on glacial meltwater chemistry, and the potential

Table 1 Concentrations of major elements (average values of duplicate analyses), TC, TN, and TS in core Mw5S from L. Maruwan

Depth (cm)	Mid-depth	MgO (wt%)	Al ₂ O ₃	SiO ₂	K ₂ O	CaO	TiO ₂	MnO	Fe ₂ O ₃	Carbon (wt%)	Nitrogen	Sulfur	C/N	¹⁴ C age (years BP)	1σ	δ ¹³ C (‰ vs. PDB)	δ ¹⁵ N (‰ vs. Air)
0 to 2	1.0	3.0	10.5	46.6	3.4	2.8	0.91	0.17	7.5	1.3	0.00	0.3	-	1,350	40	-18.0	+6.6 (n = 2)
2 to 4	3.0	2.4	9.1	53.4	2.9	2.8	0.78	0.11	6.5	1.6	0.00		-				
4 to 6	5.0	0.5	4.1	67.6	1.6	2.1	0.35	0.05	3.9	2.5	0.30	1.2	8.5				+4.3 (n = 2)
6 to 8	7.0	0.0	3.2	67.2	1.4	1.9	0.30	0.05	3.7	2.8	0.36		7.9	3,950	30	-21.6	+3.1
8 to 10	9.0	0.7	5.9	59.3	2.2	2.5	0.50	0.07	5.0	2.3	0.27	1.6	8.7				
10 to 12	11.0	1.8	6.9	58.9	2.2	2.7	0.50	0.07	4.8	2.0	0.24		8.3	4,200	30	-20.8 (n = 2)	+4.9 (n = 2)
12 to 13	12.5	1.4	6.2	60.7	1.9	2.6	0.43	0.07	4.3	1.9	0.23	1.2	8.1				
13 to 14	13.5	1.3	5.4	63.7	1.7	2.4	0.39	0.06	4.0	2.0	0.26		7.5				
14 to 16	15.0	1.7	7.0	58.3	1.9	2.9	0.45	0.07	4.8	0.7	0.00	1.1	-			-19.3	+5.9
16 to 18	17.0	0.0	2.0	67.2	1.0	1.8	0.21	0.04	3.0	2.3	0.27		8.7				
18 to 20	19.0	0.0	2.1	74.4	1.1	1.9	0.24	0.04	3.2	2.4	0.30	1.0	8.1	3,920	40	-23.6	+3.2
20 to 22	21.0	0.1	1.9	74.6	1.1	1.8	0.23	0.04	3.3	2.8	0.35		8.0				
22 to 24	23.0	0.3	3.8	65.8	1.5	2.1	0.31	0.05	3.9	3.1	0.37	1.5	8.5				
24 to 26	25.0	0.3	3.6	66.6	1.5	2.1	0.31	0.05	3.6	2.2	0.24		9.2	4,410	30	-20.5	+2.2
26 to 28	27.0	0.2	3.3	70.9	1.4	2.0	0.29	0.05	3.6	3.2	0.38	1.3	8.3				
28 to 30	29.0	0.0	1.4	74.7	0.9	1.6	0.22	0.04	2.6	3.0	0.36		8.2			-21.0	+4.3
30 to 32	31.0	0.0	0.9	67.3	0.7	1.5	0.13	0.05	2.8	2.7	0.35	1.1	7.8				
32 to 34	33.0	0.0	3.0	64.6	1.3	2.0	0.30	0.06	3.7	2.4	0.30		8.0	4,630	30	-21.0	+4.8
34 to 36	35.0	0.0	3.9	65.8	1.6	2.1	0.32	0.06	3.8	2.6	0.36	1.5	7.1			-20.9	+5.1
36 to 38	37.0	0.0	2.8	69.6	1.3	2.0	0.28	0.05	3.8	3.0	0.39		7.6				
38 to 40	39.0	0.1	3.1	71.9	1.3	2.0	0.30	0.05	3.7	2.4	0.32	1.1	7.5				
40 to 43	41.5	0.0	2.6	73.4	1.2	1.9	0.26	0.04	3.3	2.9	0.40		7.2			-20.4	+4.2 (n = 2)
43 to 46	44.5	0.0	2.7	60.8	1.2	1.9	0.23	0.04	2.8	2.6	0.36	1.3	7.1				
46 to 49	47.5	0.6	4.4	65.6	1.7	2.1	0.37	0.06	3.6	3.5	0.43		8.0	4,540	40		
49 to 52	50.5	1.0	6.1	62.6	2.0	2.3	0.46	0.06	4.0	2.7	0.31	1.0	8.8			-21.2	+5.8
52 to 55	53.5	1.1	6.8	59.0	2.2	2.5	0.51	0.07	4.2	2.3	0.28		8.1				
55 to 58	56.5	2.6	8.3	55.2	2.6	2.7	0.64	0.08	4.6	1.9	0.22	0.8	8.7				
58 to 61	59.5	1.8	8.1	55.6	2.6	2.7	0.62	0.08	4.5	2.4	0.24		9.9			-21.1	+5.7
61 to 64	62.5	0.2	3.3	72.0	1.3	1.9	0.27	0.05	2.9	2.8	0.36	0.9	7.9				
64 to 67	65.5	0.0	1.3	76.4	0.9	1.6	0.17	0.04	2.8	3.1	0.43		7.3				
67 to 70	68.5	0.0	1.5	76.4	0.9	1.7	0.18	0.04	2.8	3.0	0.40	1.1	7.6			-21.2	+5.4

Table 1 Concentrations of major elements (average values of duplicate analyses), TC, TN, and TS in core Mw5S from L. Maruwan (Continued)

70 to 75	72.5	0.0	0.7	79.0	0.7	1.5	0.14	0.03	2.1	3.8	0.50		7.7	5,220	40		
75 to 80	77.5	0.0	0.5	78.5	0.6	1.5	0.12	0.03	2.0	2.8	0.34	0.7	8.4				
80 to 85	82.5	0.0	0.4	80.9	0.6	1.4	0.10	0.03	1.7	3.3	0.48		6.9			-20.6	+4.9
85 to 90	87.5	0.0	0.0	83.2	0.4	1.4	0.07	0.02	1.4	3.1	0.38	0.6	8.2				
90 to 95	92.5	0.0	0.3	82.1	0.5	1.4	0.09	0.02	1.6	2.9	0.35		8.3	5,520	90	-21.2	
95 to 100	97.5	0.0	0.2	80.9	0.6	1.5	0.11	0.03	1.7	3.1	0.37	0.7	8.3			-21.8	+4.5
100 to 105	102.5	0.0	1.0	77.4	0.8	1.6	0.15	0.03	2.2	3.1	0.39		7.8				
105 to 110	107.5	0.0	0.8	78.5	0.8	1.6	0.14	0.03	2.0	2.8	0.35	0.8	7.9	5,400	30	-20.9	
110 to 115	112.5	0.0	0.3	79.4	0.7	1.6	0.12	0.03	2.0	3.2	0.40		8.0				
115 to 120	117.5	0.0	0.4	80.6	0.6	1.5	0.11	0.03	1.7	3.0	0.40	0.8	7.6			-20.9	+4.2
120 to 125	122.5	0.0	0.6	80.7	0.6	1.4	0.11	0.02	1.6	3.3	0.44		7.5				
125 to 130	127.5	0.0	0.3	81.7	0.5	1.4	0.10	0.02	1.4	3.1	0.42	0.7	7.4	5,350	40	-17.0	+2.4
130 to 135	132.5	0.0	1.7	75.3	0.9	1.7	0.18	0.04	2.3	2.6	0.32		8.2				
135 to 140	137.5	0.0	1.7	76.0	0.9	1.7	0.18	0.03	2.3	2.7	0.34	0.9	7.9				
140 to 145	142.5	0.0	1.0	79.1	0.7	1.6	0.13	0.03	1.9	2.8	0.38		7.3				
145 to 150	147.5	0.0	1.2	77.7	0.9	1.8	0.17	0.04	2.4	2.4	0.31	0.8	7.8				
150 to 156	153.0	0.0	0.6	79.8	0.7	1.6	0.12	0.03	1.8	2.7	0.33		8.3	6,010	70	-21.4 (n = 2)	+4.5

Radiocarbon (^{14}C age), carbon, and nitrogen isotopic compositions at corresponding depths are also shown.

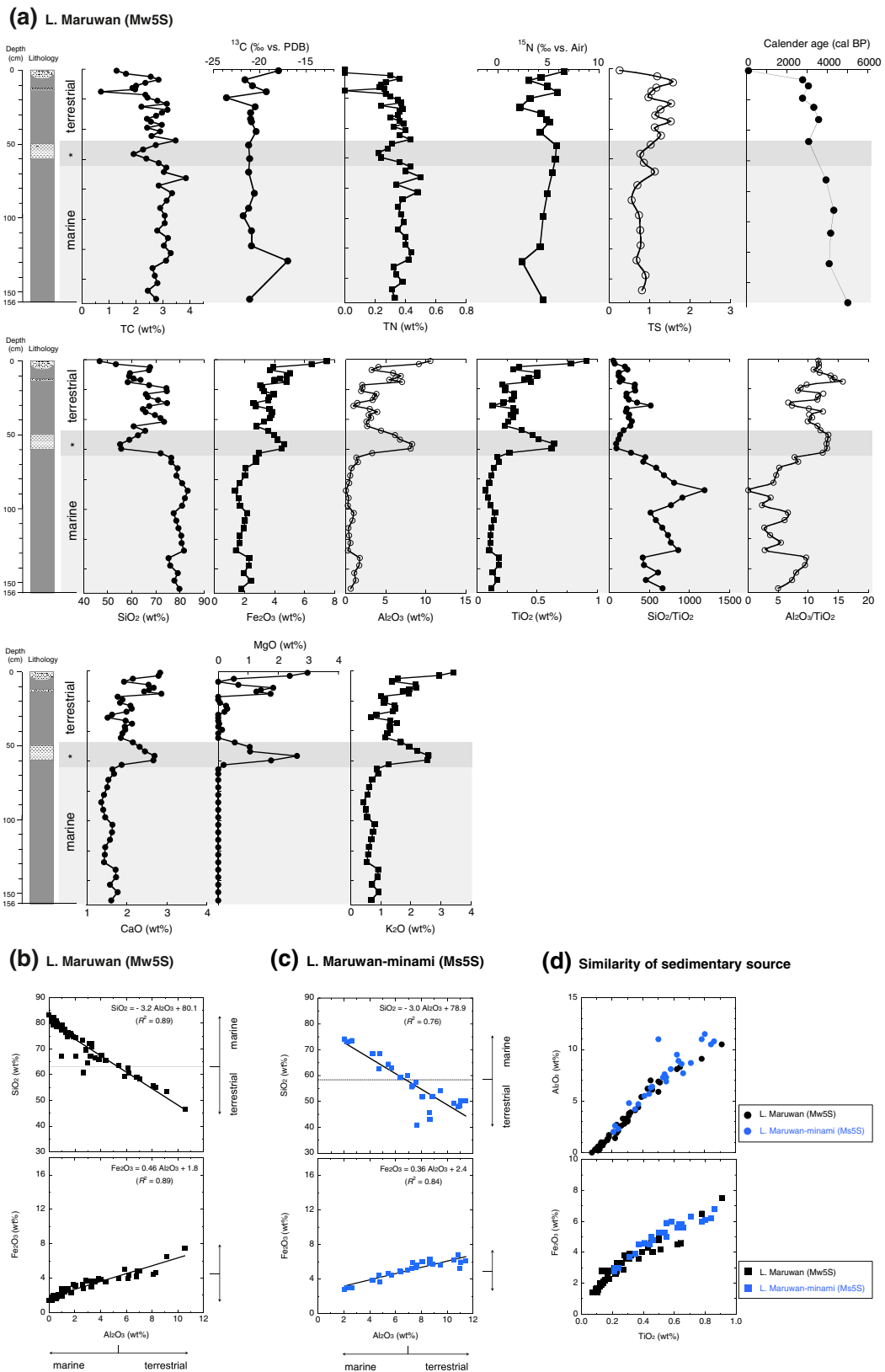


Figure 4 (See legend on next page.)

(See figure on previous page.)

Figure 4 Vertical profiles of some major elements, SiO₂-Al₂O₃ and SiO₂-Fe₂O₃ diagrams, bivariate TiO₂-Al₂O₃ and TiO₂-Fe₂O₃ plots. **(a)** Vertical profiles of lithologies, total carbon (TC), δ¹³C_{org} (‰ vs PDB), total nitrogen (TN), δ¹⁵N (‰ vs air), total sulfur (TS), ¹⁴C ages, wt% of major elements (SiO₂, Fe₂O₃, Al₂O₃, TiO₂, CaO, MgO, K₂O), and major elemental ratios (SiO₂/TiO₂ and Al₂O₃/TiO₂) in core Mw5S from L. Maruwan, showing the transition between the marine and terrestrial stages *via* possible brackish conditions (*based on microflora differences at a depth of 60 cm, determined with a DGGE analysis). The raw data are provided in Table 1. **(b), (c)** Al₂O₃-SiO₂ and Al₂O₃-Fe₂O₃ diagrams for L. Maruwan (core Mw5S) and Maruwan-minami (core Ms5S) sediments. Possible end-members of marine and terrestrial major elements are noted on the axes. **(d)** The similarity of the source rocks of L. Maruwan (core Mw5S, black symbols: R² = 0.97 and 0.92) and L. Maruwan-minami (core Ms5S, blue symbols: R² = 0.85 and 0.89) was confirmed with bivariate TiO₂-Al₂O₃ and TiO₂-Fe₂O₃ plots.

concentrations are constant throughout the core at 10.5% (representing the freshwater end-member) and (ii) SiO₂ is contained in both the biogenic and detrital components (of glacial inorganic origin), with SiO₂ concentrations in the detritus constant at 46.6% (representing the freshwater end-member). Therefore,

$$\text{Total silica}(\%) = \text{Biogenic silica}(\%) + \text{Detrital silica}(\%)$$

where the detrital ratio of the end-member (Figure 4b,c) is as follows:

$$\frac{\text{Detrital silica}(\%)}{\text{Detrital Al}_2\text{O}_3(\%)} = \frac{46.6(\%)}{10.5(\%)}$$

Hence, for L. Maruwan:

$$\text{Biogenic silica}(\%) = \text{Total silica}(\%) - 4.43 \text{ Detrital Al}_2\text{O}_3(\%)$$

and in L. Maruwan-minami:

$$\text{Biogenic silica}(\%) = \text{Total silica}(\%) - 4.36 \text{ Detrital Al}_2\text{O}_3(\%)$$

Based on the TiO₂-normalized plots of Al₂O₃ and Fe₂O₃, the similarity of the source rocks in the two lakes is high (Figure 4d), suggesting the discharge of homogenous meltwater into both lakes.

Figure 5a shows the depth profiles of the reconstructed biogenic silica concentrations in L. Maruwan. After the marine-terrestrial transition, diatoms were the main primary producers, even in the freshwater/brackish environments. Based on the DGGE and molecular analyses, the major phototrophic producers were identical to those detected in the deeper sediment layers of L. Skallen (i.e., diatoms) (Takano *et al.* 2012). Therefore, the origin of Si in the Antarctic lakes is of particular interest because dissolved silica is essential for the growth of diatoms (i.e., diatoms are the dominant group of phytoplankton with amorphous opal constituents).

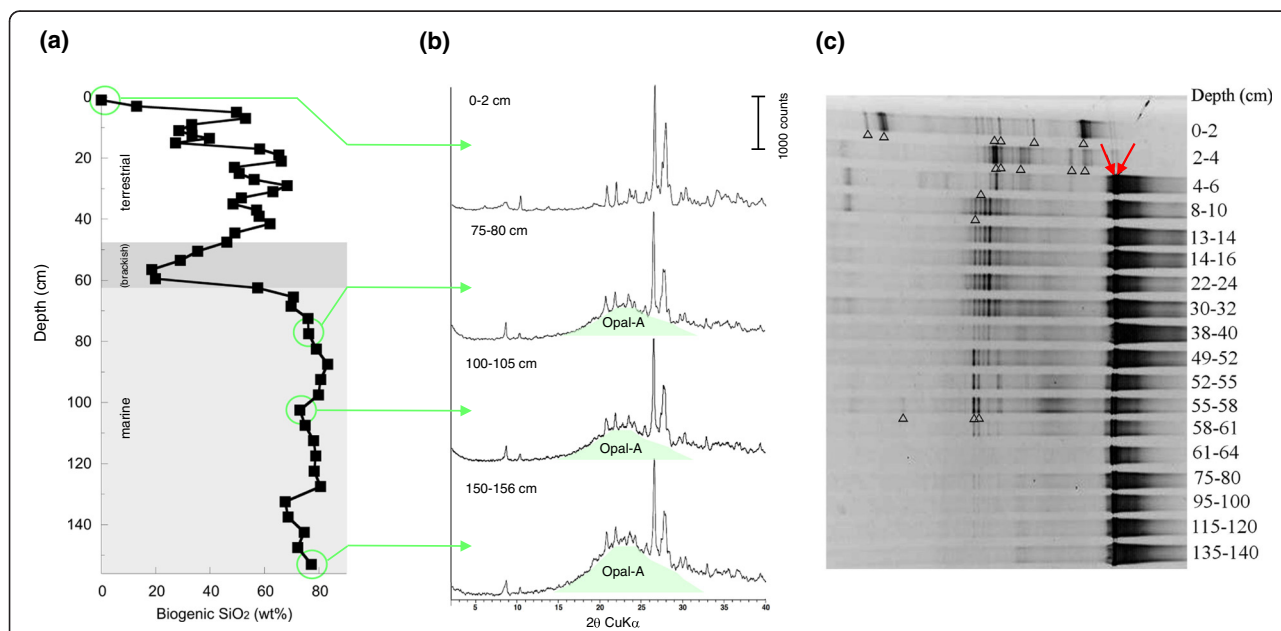


Figure 5 Depth profiles of biogenic silica concentrations and X-ray diffraction analyses of sediments from core Mw5S. **(a)** Vertical profiles of biogenic silica content (wt%), **(b)** opal-A signatures determined with X-ray diffraction analysis, and **(c)** denaturing gradient-gel electrophoresis (DGGE) analysis of L. Maruwan sediments (core Mw5S). Note that the direction of electrophoresis is from right to left.

Table 2 Radiocarbon (^{14}C) age data obtained with AMS for the organic carbon fractions from core Mw5S from L. Maruwan

Depth (cm)	Mid-depth	Conventional radiocarbon age ($\delta^{13}\text{C}$ corrected) (years BP)	1σ \pm	Calendar age (2σ range) (cal BP)	Relative area under probability function
0 to 2	1.0	1,350	40	24 to 141	0.73
				220 to 262	0.25
6 to 8	7.0	3,950	30	2,737 to 2,798	0.93
				2,819 to 2,844	0.06
10 to 12	11.0	4,200	30	2,950 to 3,160	1.00
18 to 20	19.0	3,920	40	2,706 to 2,813	0.94
				2,816 to 2,844	0.03
				2,618 to 2,633	0.03
24 to 26	25.0	4,410	30	3,256 to 3,392	1.00
32 to 34	33.0	4,630	30	3,475 to 3,637	1.00
46 to 49	47.5	4,540	40	3,382 to 3,560	1.00
70 to 75	72.5	5,220	40	3,790 to 4,053	1.00
90 to 95	92.5	5,520	90	4,056 to 4,565	1.00
105 to 110	107.5	5,400	30	4,042 to 4,274	1.00
125 to 130	127.5	5,350	40	3,950 to 4,218	1.00
150 to 156	153.0	6,010	70	4,807 to 5,204	1.00

Conventional radiocarbon dating based on organic carbon values ($^{14}\text{C}_{\text{org}}$, years BP) was corrected for the marine reservoir effect ($\Delta R = 1,300$ years for the marine stage sequence) using core-top data. Calendar age data were calculated using the calibration programs Calib Rev 6.0.1 (Stuiver and Reimer 1993; Stuiver *et al.* 1998), INTCAL09 and MARINE09 (e.g., Hughen *et al.* 2004; Reimer *et al.* 2004, 2009). See discussions of the biogeochemical recycling processes for relic carbon in the Antarctic region (e.g., Ingolfsson *et al.* 1998; Berkman *et al.* 1998) and the Soya Coast region (e.g., Miura *et al.* 2002).

Subglacial abrasion and weathering cause continuous input of silica

Sawagaki and Hirakawa (1997) have described the formation of glacial erosional bedforms in the Rundvågshetta area. The erosional bedforms are accompanied by small erosional marks, which support the interpretation that subglacial meltwater has contributed to the erosion at the base of Antarctic glaciers (cf. Figure 6). It is important to note that some subglacial erosional features may have resulted from subglacial streams, as shown in Figure 2d. Anderson *et al.* (2002) have extensively reviewed the features of subglacial meltwater drain channels beneath continental ice sheets. Observations and interpretations of these bedforms have been used to reconstruct the historical development of glacial erosional bedforms (e.g., Shaw 2002), and to understand the significance and implications of subglacial water-rock interactions. Further support for this finding comes from the cosmogenic radionuclide dating of local glacial erratics and bedrock (Yamane *et al.* 2011). Both bedrocks and erratics show similar exposure ages, suggesting the presence of warm basal ice during the last glacial period, which would have included subglacial water channels.

We suggest that the continuous input of subglacial meltwater influenced the chemical compositions of areas marginal to the ice sheet (also, see de Mora *et al.* 1994;

Brown 2002). Nelson and Treguer (1992) reported that silicon is an important limiting nutrient for Antarctic diatom productivity. Total biogenic silica (%) and total carbon contents are positively correlated in L. Maruwan ($R = 0.75$; this study). When inferring the past constraints on the primary production by diatoms in the ice-marginal lakes, we concluded that the subglacial weathering of silicate and aluminosilicate minerals supplied significant levels of minerals, nitrogen, and relic carbon to subglacial meltwaters (e.g., Hutchins and Bruland 1998). Therefore, dissolved inorganic silicates are constantly available for utilization by the diatom communities that are the primary producers in the perennially ice-covered lakes at Rundvågshetta.

Conclusions

- [1] This study provides the first published data on the subglacial limnology and Si biogeochemistry of L. Maruwan, Rundvågshetta. The reservoir effects of relic carbon derived from the subglacial water beneath the Rundvåg Glacier were estimated at 1,300 years (cf. core-top age 1,350 years in Mw5S). The nitrogen isotopic composition of the bulk sediment was slightly ^{15}N -enriched relative to the dinitrogen in atmospheric air, even in freshwater

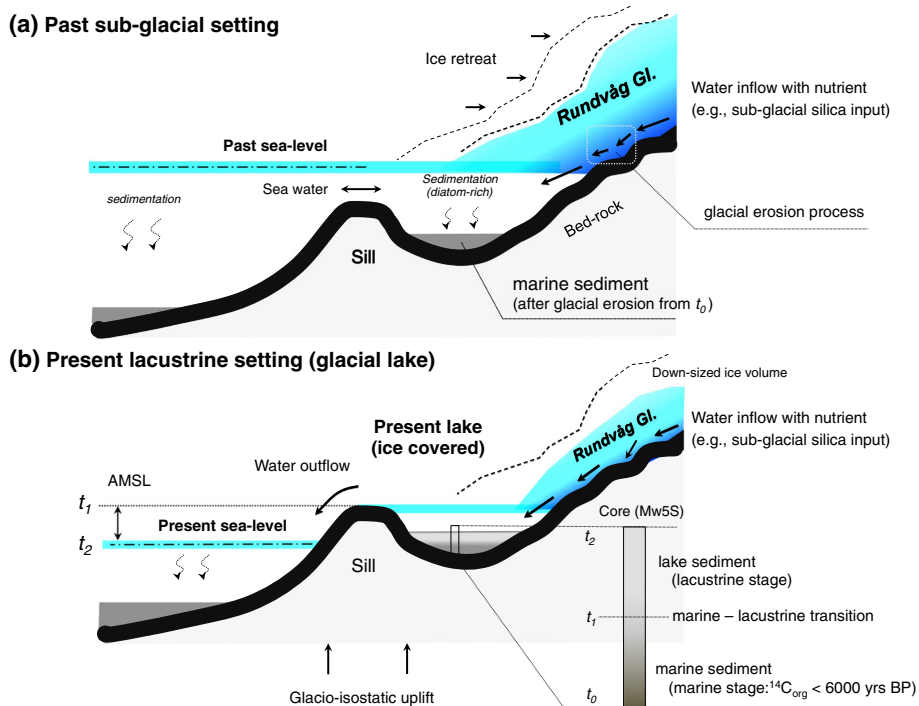


Figure 6 Inflow of subglacial meltwater containing solid-phase materials and dissolved nutrients, including silica, relic carbon, and nitrogen. Schematic models of (a) past lake setting after glacial erosion (i.e., the initiation of sedimentation processes during the marine phase) and (b) present lake setting (lacustrine stage). The relative sea level is controlled by glacio-isostatic uplift. For the present sea ice conditions during the summer season (December 2005; photograph taken from a helicopter), please see the description of the landscape of Rundvågshetta (Additional file 1).

environments (cf. sedimentary $\delta^{15}\text{N}$ in freshwater at L. Skallen). Based on the similarities in the compositions of their major sedimentary elements, lakes Maruwan and Maruwan-minami share the same meltwater source composition.

[2] We suggest that the amount of bioavailable silica flowing out from subglacial drainage channels under the EAIS and into subglacial and proglacial lakes in the area is extremely limited, underscoring the biological significance of subglacial physicochemical weathering and water-rock interactions. Inorganic Si is the main source of biogenic silica (up to 83 wt%) for lacustrine diatom communities, indicating the strong relationship between the subglacial material exported from the glacial system and the primary production in these glacial lakes during the Holocene.

Additional file

Additional file 1: Supplementary Information. Biogeochemistry and limnology in Antarctic subglacial weathering: Molecular evidence of the linkage between subglacial silica input and primary producers in a perennially ice-covered lake.

Abbreviations

EAIS: East Antarctic Ice Sheet; WAIS: West Antarctic Ice Sheet; LHB: Lützow-Holm Bay; AMSL: above the mean sea level; opal-A: amorphous hydrated silica; AMS: accelerator mass spectrometry; XRF: X-ray fluorescence; XRD: X-ray diffraction; PCR: polymerase chain reaction; DGGE: denaturing gradient gel electrophoresis.

Competing interests

The authors declare that they have no competing interests.

Authors' contributions

YT compiled the geochemical data and wrote the paper. HK and ET contributed to the molecular analysis. YY supported the radiocarbon analysis. YT and MF performed the field investigations and designed the entire research project, in discussion with the coauthors. All authors read and approved the final manuscript.

Authors' information

YT is a senior research scientist at the Department of Biogeochemistry, Japan Agency for Marine-Earth Science and Technology (JAMSTEC). HK is an assistant professor at the Institute of Low Temperature Science, Hokkaido University. ET was a graduate school student at the Institute of Low Temperature Science, Hokkaido University. YY is a professor at the Atmosphere and Ocean Research Institute (AORI), University of Tokyo. MF is a professor at the Institute of Low-Temperature Science, Hokkaido University.

Acknowledgements

We thank J. Sickman (Univ. California, Riverside), J. Tyler (Univ. Adelaide), and an anonymous reviewer for critical and constructive comments which helped to improve an earlier version of the manuscript. We also thank T. Sato (Hiroshima Univ.) and S. Imura (Natl. Inst. Polar Res., NIPR) for logistical

supports, T. Sawagaki (Hokkaido Univ.) for the onsite field guide regarding past glacial erosion processes, N. Suzuki (Hokkaido Univ.) and N. Ohkouchi (JAMSTEC) for discussions, and members of the 47th Japan Antarctica Research Expedition (Expedition Leader: K. Shiraiishi, NIPR) for logistical assistance. The AMS experiments were partially supported by Dr. H. Matsuzaki (Univ. Tokyo). Part of this work has been presented at the AGU Chapman Conference 2010 on the Exploration and Study of Antarctic Subglacial Aquatic Environment at Baltimore, USA. This research was supported in part by the Japan Society for the Promotion of Science (Y.T.) and NEXT program No. GR031 (Y.Y.).

Author details

¹Department of Biogeochemistry, Japan Agency for Marine-Earth Science and Technology (JAMSTEC), 2-15 Natsushima, Yokosuka, Kanagawa 237-0061, Japan.

²The Institute of Low Temperature Science, Hokkaido University, N19, W8, Kita-ku, Sapporo, Hokkaido 060-0819, Japan. ³Atmosphere and Ocean Research Institute, University of Tokyo, 5-1-5 Kashiwanoha, Kashiwa, Chiba 277-8564, Japan.

Received: 29 September 2014 Accepted: 17 February 2015

Published online: 15 April 2015

References

- Anderson JB, Shipp SS, Lowe AL, Wellner JS, Mosola AB (2002) The Antarctic ice sheet during the Last Glacial Maximum and its subsequent retreat history: a review. *Quaternary Sci Rev* 21:49–70
- Bassett S, Milne G, Bentley M, Huybrechts P (2007) Modelling Antarctic sea-level data to explore the possibility of a dominant Antarctic contribution to meltwater pulse IA. *Quaternary Sci Rev* 26:2113–2127
- Bentley M, Christoffersen P, Hodgson D, Smith AM, Tulaczyk S, Le Brocq A (2011) Subglacial lake sediments and sedimentary processes: potential archives of ice sheet evolution, past environmental change, and the presence of life. *Geophys Monogr Ser* 192:83–110
- Berkman PA, Forman SL (1996) Pre-bomb radiocarbon and the reservoir correction for calcareous marine species in the Southern Ocean. *Geophys Res Lett* 23:363–366
- Berkman PA, Andrews JT, Björck S, Colhoun EA, Emslie SD, Goodwin ID, Hall BL, Hart CP, Hirakawa K, Igarashi A, Ingolfsson O, Lopez-Martinez J, Lyons WB, Mabin MCG, Quilty PG, Taviani M, Yoshida Y (1998) Circum-Antarctic coastal environmental shifts during the Late Quaternary reflected by emerged marine deposits. *Antarctic Sci* 10:345–362
- Brown GH (2002) Glacier meltwater hydrochemistry. *Appl Geochem* 17:855–883
- Christner BC, Royston-Bishop G, Foreman CM, Arnold BR, Tranter M, Welch KA, Lyons WB, Tsapin AI, Studinger M, Priscu JC (2006) Limnological conditions in subglacial Lake Vostok, Antarctica. *Limnol Oceanogr* 51:2485–2501
- Cox R, Culkin F, Riley J (1967) The electrical conductivity/chlorinity relationship in natural sea water. *Deep Sea Res Oceanogr Abstr* 14:203–220
- de Mora SJ, Whitehead R, Gregory M (1994) The chemical composition of glacial melt water ponds and streams on the McMurdo Ice Shelf, Antarctica. *Antarctic Sci* 6:17–27
- Esposito R, Horn S, McKnight D, Cox M, Grant M, Spaulding S, Doran P, Cozzetto K (2006) Antarctic climate cooling and response of diatoms in glacial meltwater streams. *Geophys Res Lett* 33:L07406
- Geographical Survey Institute (1984) Rundvågshetta: the principal part. Map compilation from air photography, controlled by triangulation points established by JARE, 1971 and 1974
- Hodgson DA, Verleyen E, Squier AH, Sabbe K, Keely BJ, Saunders KM, Vyverman W (2006) Interglacial environments of coastal east Antarctica: comparison of MIS 1 (Holocene) and MIS 5e (Last Interglacial) lake-sediment records. *Quaternary Sci Rev* 25:179–197
- Hodgson DA, Roberts SJ, Bentley MJ, Smith JA, Johnson JS, Verleyen E, Vyverman W, Hodson AJ, Leng MJ, Cziferszky A, Fox AJ, Sanderson DCW (2009) Exploring former subglacial Hodgson Lake, Antarctica Paper I: site description, geomorphology and limnology. *Quaternary Sci Rev* 28:2295–2309
- Hodson A (2006) c. *Water Resource Res* 42, W11406. doi:11410.11029/12005WR004311
- Hodson A, Heaton T, Langford H, Newsham K (2010) Chemical weathering and solute export by meltwater in a maritime Antarctic glacier basin. *Biogeochem* 98:9–27
- Hughen KA, Baillie MGL, Bard E, Beck JW, Bertrand CJH, Blackwell PG, Buck CE, Burr GS, Cutler KB, Damon PE, Edwards RL, Fairbanks RG, Friedrich M, Guilderson TP, Kromer B, McCormac G, Manning S, Ramsey CB, Reimer PJ, Reimer RW, Remmele S, Southon JR, Stuiver M, Talamo S, Taylor FW, der Plicht J, Weyhenmeyer CE (2004) Marine04 marine radiocarbon age calibration, 0–26 cal kyr BP. *Radiocarbon* 46:1059–1086
- Hutchins DA, Bruland KW (1998) Iron-limited diatom growth and Si:N uptake ratios in a coastal upwelling regime. *Nature* 393:561–564
- Imai N, Terashima S, Itoh S, Ando A (1995) 1994 compilation values for GSJ reference samples, igneous rock series. *Geochem J* 29:91–95
- Imai N, Terashima S, Itoh S, Ando A (1999) 1998 compilation of analytical data for five GSJ geochemical reference samples. *Geostandards Newslett* 23:223–250
- Imura S, Bando T, Seto K, Ohtani S, Kudoh S, Kanda H (2003) Distribution of aquatic mosses in the Soya Coast region, East Antarctica. *Polar Biosci* 16:1–10
- Ingolfsson O, Hjort C, Berkman PA, Björck S, Colhoun E, Goodwin ID, Hall B, Hirakawa K, Melles M, Moller P, Prentice ML (1998) Antarctic glacial history since the Last Glacial Maximum: an overview of the record on land. *Antarctic Sci* 10:326–344
- Jouzel J, Petit J, Souchez R, Barkov N, Lipenkov V, Raynaud D, Stievenard M, Vassiliev N, Verbeke V, Vimeux F (1999) More than 200 meters of lake ice above subglacial Lake Vostok, Antarctica. *Science* 286:213–214
- Kapitsa A, Ridley J, Robin G, Siegert M, Zotikov I (1996) A large deep freshwater lake beneath the ice of central East Antarctica. *Nature* 381:684–686
- Karl DM, Bird DF, Björckman K, Houlihan T, Shackelford R, Tupas L (1999) Microorganisms in the accreted ice of Lake Vostok, Antarctica. *Science* 286:2144–2147
- Kastner M, Keene J, Gieskes J (1977) Diagenesis of siliceous oozes - I. Chemical controls on the rate of opal-A to opal-CT transformation - an experimental study. *Geochim Cosmochim Acta* 41:1041–1059
- Koblinsky C, Hildebrand P, LeVine D, Pellerano F, Chao Y, Wilson W, Yueh S, Lagerloef G (2003) Sea surface salinity from space: science goals and measurement approach. *Radio Sci* 38:8064, 10.1029/2001RS002584
- Kudoh S, Tanabe Y (2014) Limnology and ecology of lakes along the Soya Coast, East Antarctica. *Adv Polar Sci* 25:75–91
- Lee K, Tong LT, Millero FJ, Sabine CL, Dickson AG, Goyet C, Park GH, Wanninkhof R, Feely RA, Key RM (2006) Global relationships of total alkalinity with salinity and temperature in surface waters of the world's oceans. *Geophys Res Lett* 33:L19605, 10.1029/2006GL027207
- Leng MJ, Barker PA (2006) A review of the oxygen isotope composition of lacustrine diatom silica for palaeoclimate reconstruction. *Earth-Sci Rev* 75:5–27
- Matsumoto G, Tani Y, Seto K, Tazawa T, Yamamuro M, Watanabe T, Nakamura T, Takemura T, Imura S, Kanda H (2010) Holocene paleolimnological changes in Lake Skallen Oike in the Syowa Station area of Antarctica inferred from organic components in a sediment core (Sk4C-02). *J Paleolimnol* 44:677–693
- Matsumoto G, Honda E, Seto K, Tani Y, Watanabe T, Ohtani S, Kashima K, Nakamura T, Imura S (2014) Holocene paleolimnological changes of Lake Oyako-ike in the Soya Kaigan of East Antarctica. *Inland Waters* 4:105–112
- Mikucki JA, Pearson A, Johnston DT, Turchyn AV, Farquhar J, Schrag DP, Anbar AD, Priscu JC, Lee PA (2009) A contemporary microbially maintained subglacial ferrous "Ocean". *Science* 324:397–400
- Miura H, Maemoku H, Igarashi A, Moriwaki K (1998) Late Quaternary raised beach deposits and radiocarbon dates of marine fossils around Lützow-Holm Bay. Special map series of National Institute of Polar Research, pp. 1–46
- Miura H, Maemoku H, Moriwaki K (2002) Holocene raised beach stratigraphy and sea-level history at Kizhashi Beach, Skarvsnes, Lutzow-Holm Bay, Antarctica. *Royal Soc New Zealand Bull* 35:391–396
- Murayama H (1977) General characteristics of the Antarctic lakes near Syowa station. *Antarctic Record* 58:43–62
- Muyzer G, Brinkhoff T, Nübel U, Santegoeds C, Schafer H, Wawer C (1996) Denaturing gradient gel electrophoresis (DGGE) in microbial ecology. In: Akkermans ADL, van Elsas JD, de Bruijn FJ (eds) *Molecular microbial ecology manual*, 3rd edn. Kluwer Academic Publishers, Dordrecht, The Netherlands, pp 1–27, p. 3.4.4
- Nelson D, Treguer P (1992) Role of silicon as a limiting nutrient to Antarctic diatoms: evidence from kinetic studies in the Ross Sea ice-edge zone. *Mar Ecol Progr Ser* 80:255–264
- Oswald G, Robin GQ (1973) Lakes beneath the Antarctic ice sheet. *Nature* 245:251–254
- Oyama M, Takehara H (2005) Revised Standard Soil Color Charts: 27th edition (ed. The Ministry of Agriculture, Forestry and Fisheries of Japan)
- Priscu JC, Adams EE, Lyons WB, Voytek MA, Mogk DW, Brown RL, McKay CP, Takacs CD, Welch KA, Wolf CF, Kirshtein JD, Avci R (1999) Geomicrobiology of subglacial ice above Lake Vostok, Antarctica. *Science* 286:2141–2144

- Raiswell R (1984) Chemical models of solute acquisition in glacial meltwaters. *J Glaciol* 30:49–57
- Raiswell R, Canfield DE (2012) The iron biogeochemical cycle past and present. *Geochem Perspect* 1:1–322
- Reimer PJ, Baillie MGL, Bard E, Bayliss A, Beck JW, Bertrand CJH, Blackwell PG, Buck CE, Burr GS, Cutler KB, Damon PE, Edwards RL, Fairbanks RG, Friedrich M, Guilderson TP, Hogg AG, Hughen KA, Kromer B, McCormac G, Manning S, Ramsey CB, Reimer RW, Remmele S, Southon JR, Stuiver M, Talamo S, Taylor FW, van der Plicht J, Weyhenmeyer CE (2004) IntCal04 terrestrial radiocarbon age calibration, 0–26 cal kyr BP. *Radiocarbon* 46:1029–1058
- Reimer PJ, Baillie MG, Bard E, Bayliss A, Beck JW, Blackwell PG, Bronk RC, Buck CE, Burr GS, Edwards RL (2009) IntCal09 and Marine09 radiocarbon age calibration curves 0–50,000 years cal BP. *Radiocarbon* 51:1111–1150
- Robin GQ, Swithinbank C, Smith B (1970) Radio echo exploration of the Antarctic ice sheet. *Inter Assoc Sci Hydrol Publ* 86:97–115
- Satish-Kumar M, Wada H (2000) Carbon isotopic equilibrium between calcite and graphite in Skallen Marbles, East Antarctica: Evidence for the preservation of peak metamorphic temperatures. *Chem Geol* 166:173–182
- Sawagaki T, Hirakawa K (1997) Erosion of bedrock by subglacial meltwater. *Geografiska Annaler Series a—Phys Geogr* 79A, Soya Coast, East Antarctica, pp 223–238
- Shaw J (2002) The meltwater hypothesis for subglacial bedforms. *Quaternary Inter* 90:5–22
- Shiraishi K, Hiroi Y, Motoyoshi Y (1987) Plate tectonic development of Late Proterozoic paired metamorphic complexes in eastern Queen Maud Land, East Antarctica. *Geophys Monogr Ser* 40:309–318
- Siegert M (2000) Antarctic subglacial lakes. *Earth-Sci Rev* 50:29–50
- Siegert MJ, Dowdeswell J, Gorman M, McIntyre N (1996) An inventory of Antarctic subglacial lakes. *Antarctic Sci* 8:281–286
- Siegert MJ, Carter S, Tabacco I, Popov S, Blankenship DD (2005) A revised inventory of Antarctic subglacial lakes. *Antarctic Sci* 17:453–460
- Siegert MJ, Royston-Bishop G, Woodward J (2012) Antarctic subglacial lakes. *Encyclopedia of lakes and reservoirs*. Springer, London, pp 37–39
- Stuiver M, Reimer PJ (1993) Extended ^{14}C data base and revised Calib 3.0 ^{14}C age calibration program. *Radiocarbon* 35:215–230
- Stuiver M, Reimer PJ, Braziunas TF (1998) High-precision radiocarbon age calibration for terrestrial and marine samples. *Radiocarbon* 40:1127–1151
- Stumpf A, Elwood Madden M, Soreghan G, Hall B, Keiser L, Marra K (2012) Glacier meltwater stream chemistry in Wright and Taylor Valleys, Antarctica: significant roles of drift, dust and biological processes in chemical weathering in a polar climate. *Chem Geol* 322:79–90
- Takano Y, Tyler JJ, Kojima H, Yokoyama Y, Tanabe Y, Sato T, Ogawa ON, Ohkouchi N, Fukui M (2012) Holocene lake development and glacial-isostatic uplift at Lake Skallen and Lake Oyako, Lützow-Holm Bay, East Antarctica: based on biogeochemical facies and molecular signatures. *Appl Geochem* 27:2546–2559
- Tayasu I, Hirasawa R, Ogawa NO, Ohkouchi N, Yamada K (2011) New organic reference materials for carbon and nitrogen stable isotope ratio measurements provided by Center for Ecological Research, Kyoto University, and Institute of Biogeosciences, Japan Agency for Marine-Earth Science and Technology. *Limnol* 12:261–266
- Tranter M, Skidmore M, Wadham J (2005) Hydrological controls on microbial communities in subglacial environments. *Hydrol Processes* 19:995–998
- Verleyen E, Hodgson DA, Sabbe K, Cremer H, Emslie SD, Gibson J, Hall B, Imura S, Kudoh S, Marshall GJ, McMinn A, Melles M, Newman L, Roberts D, Roberts SJ, Singh SM, Sterken M, Tavernier I, Verkulich S, de Vyver EV, Van Nieuwenhuyze W, Wagner B, Vyverman W (2011) Post-glacial regional climate variability along the East Antarctic coastal margin: evidence from shallow marine and coastal terrestrial records. *Earth-Sci Rev* 104:199–212
- Watanabe T, Kojima H, Takano Y, Fukui M (2013) Diversity of sulfur-cycle prokaryotes in freshwater lake sediments investigated using *aprA* as the functional marker gene. *Syst Appl Microbiol* 36:436–443
- Williams W, Sherwood J (1994) Definition and measurement of salinity in salt lakes. *International J Salt Lake Res* 3:53–63
- Wingham D, Siegert M, Shepherd A, Muir A (2006) Rapid discharge connects Antarctic subglacial lakes. *Nature* 440:1033–1036
- Yamane M, Yokoyama Y, Miura H, Maemoku H, Iwasaki S, Matsuzaki H (2011) The last deglacial history of Lutzow-Holm Bay, East Antarctica. *Journal of Quaternary Sci* 26:3–6
- Yokoyama Y, Esat TM (2011) Global climate and sea level enduring variability and rapid fluctuations over the past 150,000 years. *Oceanogr* 24:54–69
- Yokoyama Y, Miyairi Y, Matsuzaki H, Tsunomori F (2007) Relation between acid dissolution time in the vacuum test tube and time required for graphitization for AMS target preparation. *Nuclear Instr Methods Phys Res Sec B* 259:330–334
- Yoshida Y, Moriwaki K (1979) Some consideration on elevated coastal features and their dates around Syowa Station, Antarctica. *Memoirs Nat Inst Polar Res* 13:220–226
- Yoshikawa T, Toya H (1957) Report on geomorphological results of the Japanese Antarctic Research Expedition, 1956–1957. *Antarctic Record* 1:1–13
- Young GM, Nesbitt HW (1998) Processes controlling the distribution of Ti and Al in weathering profiles, siliciclastic sediments and sedimentary rocks. *J Sediment Res* 68:448–455

Submit your manuscript to a SpringerOpen® journal and benefit from:

- Convenient online submission
- Rigorous peer review
- Immediate publication on acceptance
- Open access: articles freely available online
- High visibility within the field
- Retaining the copyright to your article

Submit your next manuscript at ► springeropen.com
